*Acta Cryst.* (1992). B48, 370–376

# Crystal Chemistry of $Mg_2P_2O_7.nH_2O$, $n = 0$, 2 and 6: Magnesium–Oxygen Coordination and Pyrophosphate Ligation and Conformation

BY MOHAMED SOUHASSOU

*Université de Nancy* I, *Laboratoire de Minéralogie et Cristallographie, Boîte Postale n*° 239, 54506 *Vandoeuvre-lès-Nancy CEDEX, France, and Medical Foundation of Buffalo*, 73 *High Street, Buffalo, New York* 14203, *USA*

CLAUDE LECOMTE

*Université de Nancy* I, *Laboratoire de Minéralogie et Cristallographie, Boîte Postale n*° 239, 54506 *Vandoeuvre-lès-Nancy CEDEX, France*

AND ROBERT H. BLESSING*

*Medical Foundation of Buffalo*, 73 *High Street, Buffalo, New York* 14203, *USA*

(*Received* 1 *April* 1991; *accepted* 2 *December* 1991)

## Abstract

The crystal structure of the hexahydrate has been determined and is compared with the known structures of the dihydrate and two forms of the anhydrous compound. Comparisons among the structures provide some insight as to the structural role of $Mg^{2+}$ as a cofactor in the ATP–ADP hydrolysis reactions of bioenergetics. Crystal data for dimagnesium pyrophosphate hexahydrate: $Mg_2P_2O_7.6H_2O$, $M_r = 330.66$, monoclinic, $P2_1/n$, $a = 7.189$ (2), $b = 18.309$ (8), $c = 7.665$ (5) Å, $\beta = 92.360$ (14)°, $V = 1008.1$ Å$^3$, $Z = 4$, $D_x = 2.18$ mg mm$^{-3}$, $F(000) = 680$, $\mu = 0.609$ mm$^{-1}$ for $\lambda$(Mo $K\alpha$) = 0.7107 Å. $R(|F|) = 0.047$ for 937 data.

## Introduction

We have determined the structure of the hexahydrate, which crystallized after cation exchange between aqueous $Na_2H_2P_2O_7$ solution and $Mg^{2+}$-loaded cation-exchange resin. The structures of the dihydrate and of two phases of the anhydrous compound have been known for some time. The dihydrate (Oka & Kawahara, 1982) crystallized under hydrothermal conditions at ~700 K from a mixture of precipitated $MgHPO_4.3H_3O$ (newberyite) and $H_3PO_4$. Both anhydrous phases (Calvo, 1967, 1965; Lukaszewicz, 1967, 1961) crystallized from melts obtained after thermal decomposition of precipitated $MgNH_4PO_4.6H_2O$ (struvite). The low-temperature $\alpha$-phase and the high-temperature $\beta$-phase (isostructural with thortveitite, $Sc_2Si_2O_7$) interconvert through a diffuse phase transition and can coexist in the range 333–343 K (Calvo, 1967).

In the anhydrous structures, six terminal oxygens of the $O_3POPO_3^{4-}$ pyrophosphate anions must coordinate two $Mg^{2+}$ cations. This is achieved with the anions in staggered conformations acting as monodentate ligands. Each terminal oxygen is shared between two cations, each of which binds six oxygens, but some of the $MgO_6$ octahedra are distorted to quite irregular geometries. In the hydrated structures, the water molecules participate in the Mg—O coordination and permit more regular octahedral geometry. The anions assume eclipsed conformations to bind the aqua cations in a bidentate chelate manner, as is supposed for binding of $Mg^{2+}$ by ATP and ADP in their biological hydrolysis reactions.

## Experimental work and structure analysis

$Mg_2P_2O_7.6H_2O$ was obtained by cation exchange between an aqueous solution of commerical $Na_2H_2P_2O_7$ and a column of Dowex-50 cation-exchange resin loaded with $Mg^{2+}$. When the solution eluted from the column with water was allowed to stand in an aspirator-evacuated vacuum desiccator over anhydrous calcium sulfate, small crystals deposited. The most common habit appeared to be hexagonal platelets with edges of some 50–100 µm and perhaps 20 µm thick; on closer examination these crystals proved to be short trigonal antiprisms. One such crystal was used for the diffraction measurements.

Only limited diffractometer time was available for this study, so only a small set of diffraction data,

* To whom correspondence should be addressed.

0108-7681/92/040370-07$06.00

amounting to $\sim 50$ unique Bragg reflections per unique non-H atom, was measured. As shown below, this abbreviated data set was quite adequate for the chemical crystallographic purposes of this study. The data were measured as $\omega/2\theta$ scan profiles for $-6 \le h \le 6$, $0 \le k \le 17$, $0 \le l \le 7$, and $(\sin\theta)/\lambda \le 0.48$ Å$^{-1}$ using Zr-filtered Mo radiation on an Enraf–Nonius CAD-4 diffractometer. Scan widths were $\Delta\omega = 0.6° + 0.36°\tan\theta$, which corresponded to about twice the base width of the reflection peaks, and the scan speed was a constant $d\omega/dt = 1.26°$ min$^{-1}$, which corresponded to $\sim 120$ reflection measurements per hour. The X-ray tube take-off angle was 2.9° so that the 'fine focus' 0.4 mm × 8 mm target focal spot was effectively a 0.4 mm square source, at a radius of 216.5 mm. The diameter of the incident beam guide aperture was sufficient for a crystal of 0.4 mm diameter to have an unobstructed view of the whole effective focal spot. The detector aperture was a constant 4 (vertical) × 2 mm (horizontal) at a radius of 174 mm, which is equivalent to 1.3 (polar) × 0.65° (equatorial). Lattice parameters were determined by least-squares fit to the setting angles of 25 reflections with $\theta$ values of $\sim 10°$.

Data reduction and error analysis (Blessing, 1989) included Bayesian statistical treatment (French & Wilson, 1978) to improve the estimates of $|F|^2$, $\sigma(|F|^2)$, $|F|$, and $\sigma(|F|)$ for the weak reflections. Absorption corrections were not necessary because all transmission factors would have exceeded $A_{\min} = 0.94$. Examination of the $k|F_o| - |F_c|$ differences at the end of the structure refinement showed that extinction effects were also negligible. A total of 1090 reflection profiles were recorded. Inspection of profile plots gave $h0l$, $l + h = 2n$, and $0k0$, $k = 2n$, as the conditions for possible reflection. Of the 1036 symmetry-allowed reflections measured, 937 were unique. The $hk0$ reflections were measured as both $-hk0$ and $+hk0$, and $1\bar{2}\bar{2}$ was remeasured at 2 h intervals as a reference intensity monitor. The latter showed only random variation over the 16.4 h of X-ray exposure with $\sigma^2(|F|^2) = \sigma^2_{\text{count}} + (p|F|^2)^2$ and $p = 0.038$. Averaging the 185 equivalent or repeated measurements of 85 of the unique reflections gave $R_{\text{int}} = [\sum(|F|^2 - \langle|F|^2\rangle)^2/\sum(|F|^2)^2]^{1/2} = 0.031$. There were 757 unique data with $|F|^2 > 2\sigma(|F|^2)$, but all 937 unique data were used in the least-squares refinement.

Initially, an incorrect chemical composition $MgH_2P_2O_7$ was assumed, and an attempt at direct-methods phasing of the resulting $|E|$ amplitudes was not successful. The crystal structure was determined by Patterson search techniques based on a tetrahedral $PO_4$ fragment, and the structure analysis gave the chemical composition. Least-squares refinement minimized $\chi^2 = \sum w\Delta^2$ with $\Delta = |F_o| - |F_c|/k$ and $w = 1/\sigma^2(|F_o|)$, and converged to $R = \sum|\Delta|/\sum|F_o| = 0.047$, $wR = (\chi^2/\sum w|F_o|^2)^{1/2} = 0.048$, and $Z = [\chi^2/(n - m)]^{1/2} = 1.30$ for $n = 937$ data and $m = 193$ parameters. The refined parameters included anisotropic mean-square displacements for the non-H atoms and positions for the H atoms. Isotropic mean-square displacements for the H atoms were held fixed at calculated values $\langle u^2\rangle_H = \langle u^2\rangle_X + 0.01$ Å$^2$, where $\langle u^2\rangle_X$ is the equivalent isotropic mean-square displacement for the atom $X$ to which the H atom is covalently bound. Initial H-atom positions were found in a difference electron density map at an intermediate stage of the refinement. In a final difference map, $-0.42 < \Delta\rho < +0.38$ e Å$^{-3}$, and in the last refinement cycle, $\Delta/\sigma < 0.57$.

The *SHELX* programs (Sheldrick, 1976) were used for the structure determination, and the *NRCVAX* programs (Gabe, Lee & Le Page, 1985) were used for the final structure refinement. The analytical approximations (Cromer & Waber, 1974) to the neutral free-atom form factors for Mg, P and O, and to the spherically contracted H-atom form factor (Stewart, Davidson & Simpson, 1965) were used for the structure-factor calculations. The *ORTEP* (Johnson, 1970) and *PLUTO* (Motherwell, 1970) programs, as implemented in *NRCVAX*, and the *STRUPLO* program (Fischer, 1985) were used to prepare the crystal structure drawings.

## Results and discussion

### *The hexahydrate structure*

The structure (Tables 1 and 2 and Fig. 1) contains three types of $Mg^{2+}$ cations: Mg1 and Mg2 occupy the centers of symmetry at (0,0,0) and $(\frac{1}{2},0,\frac{1}{2})$, and Mg3 occupies a general position. All three cations are octahedrally coordinated by O atoms: Mg1 and Mg2 are both *trans*-$(H_2O)_2MgO_4$, and Mg3 is *cis*-$(H_2O)_4MgO_2$; the non-aqua O atoms are from $P_2O_7^{4-}$ pyrophosphate anions. The anions have a bent, eclipsed conformation, and each binds two Mg1 cations, each in a monodentate manner, and a pair of cations, Mg2 and Mg3, both in a bidentate, chelate manner. Each Mg1 links four different anions; each Mg2, two different anions; and each Mg3 is bound to only one anion.

All six water molecules in the structure are bound to $Mg^{2+}$ cations and are involved as donors in an intricate scheme of O—H···O—P and O—H···O—H hydrogen bonds. Five of the water oxygens and all of the pyrophosphate oxygens, including the P—O—P bridging oxygen O4, accept hydrogen bonds. Much of the hydrogen bonding is rather weak and nonspecific, and there are several three-centered O—H(···O)$_2$ bonds and bifurcated O(—H···)$_2$O bonds (Table 3). These have nonideal geometries with some O···O distances > 3 Å, H···O distances >

Table 1. *Atomic coordinates and equivalent isotropic mean-square displacements in* $Mg_2P_2O_7.6H_2O$ *crystals*

$B_{iso} = 8\pi^2(U^1 + U^2 + U^3)/3$, where the $U^i$ are the eigenvalues of the mean-square-displacement tensors $U^{ij}$ defined by $f(\mathbf{h})|_{T>0} = f(\mathbf{h})|_{T=0}\exp(-2\pi^2 \sum_{i=1}^{3} \sum_{j=1}^{3} h_i h_j a^{*i} a^{*j} U^{ij})$.

| | $x$ | $y$ | $z$ | $B_{iso}$ (Å$^2$) |
|---|---|---|---|---|
| Mg1 | 0 | 0 | 0 | 0.92 (12) |
| Mg2 | $\frac{1}{2}$ | 0 | $\frac{1}{2}$ | 1.10 (12) |
| Mg3 | 0.1946 (3) | 0.25541 (10) | 0.5264 (3) | 1.18 (10) |
| P1 | 0.20068 (21) | 0.09659 (8) | 0.69885 (20) | 0.85 (7) |
| P2 | 0.16927 (21) | 0.10375 (8) | 0.32321 (21) | 0.88 (7) |
| O1 | 0.0213 (5) | 0.07342 (19) | 0.1990 (5) | 0.98 (16) |
| O2 | 0.1799 (5) | 0.18668 (19) | 0.3132 (5) | 1.23 (20) |
| O3 | 0.2753 (5) | 0.17353 (19) | 0.6948 (5) | 1.05 (18) |
| O4 | 0.0903 (5) | 0.08423 (20) | 0.5126 (5) | 0.90 (17) |
| O5 | 0.3583 (5) | 0.06860 (20) | 0.3147 (5) | 1.16 (17) |
| O6 | 0.0575 (5) | 0.08548 (20) | 0.8320 (5) | 1.14 (18) |
| O7 | 0.3560 (5) | 0.04027 (20) | 0.7071 (5) | 0.99 (17) |
| Ow1 | 0.2907 (6) | −0.02225 (25) | 0.0255 (6) | 1.53 (21) |
| Ow2 | 0.1261 (6) | 0.33829 (23) | 0.3458 (5) | 1.65 (20) |
| Ow3 | 0.2006 (7) | 0.33456 (25) | 0.7227 (6) | 2.33 (23) |
| Ow4 | 0.4715 (6) | 0.2831 (3) | 0.4976 (6) | 1.56 (21) |
| Ow5 | 0.2982 (6) | −0.07917 (25) | 0.4558 (6) | 1.71 (20) |
| Ow6 | −0.0899 (6) | 0.2424 (3) | 0.5646 (7) | 2.17 (23) |
| H11 | 0.329 (8) | −0.004 (3) | −0.067 (8) | 2.0 |
| H12 | 0.341 (9) | −0.000 (3) | 0.096 (8) | 2.0 |
| H21 | 0.126 (8) | 0.389 (4) | 0.381 (8) | 2.4 |
| H22 | −0.002 (9) | 0.335 (3) | 0.289 (8) | 2.4 |
| H31 | 0.114 (9) | 0.359 (4) | 0.780 (9) | 3.1 |
| H32 | 0.295 (9) | 0.362 (4) | 0.758 (9) | 3.1 |
| H41 | 0.516 (10) | 0.284 (4) | 0.583 (9) | 2.3 |
| H42 | 0.511 (8) | 0.320 (3) | 0.409 (8) | 2.3 |
| H51 | 0.308 (8) | −0.114 (3) | 0.353 (8) | 2.4 |
| H52 | 0.201 (9) | −0.071 (4) | 0.460 (9) | 2.4 |
| H61 | −0.153 (9) | 0.249 (4) | 0.472 (9) | 2.8 |
| H62 | −0.155 (9) | 0.250 (3) | 0.664 (9) | 2.8 |

2 Å, and O—H···O angles < 100°. The hydrogen bonding is weak and nonspecific presumably because the crystal packing is determined by the electrostatic cation–anion interactions and $Mg^{2+}$–$OH_2$ ion–dipole interactions, rather than by directed hydrogen-bond stereochemistry, which often determines the packing in hydrogen-bonded molecular crystals.

In the $MgO_6$ octahedra, the Mg—O distances range from 2.033 to 2.131 Å. There does not appear to be any significant systematic difference between the Mg—OP and Mg—$OH_2$ distances. The *cis*

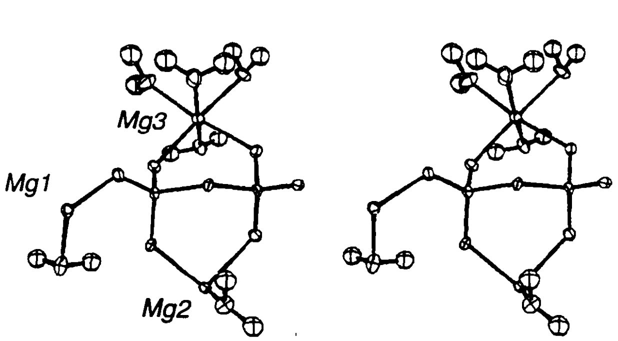


Fig. 1. The crystal-chemical unit of the $Mg_2P_2O_7.6H_2O$ structure. The Mg1 and Mg2 cations occupy inversion centers of crystallographic symmetry; the Mg3 cation occupies a general position. The ellipsoids enclose 50% probability of thermal vibrational displacement.

Table 2. *Valence geometries in* $Mg_2P_2O_7.6H_2O$ *crystals*

Bond lengths (Å)

| | | | |
|---|---|---|---|
| Mg1—O1 | 2.033 (4) | Mg2—O7 | 2.066 (4) |
| Mg1—O6 | 2.077 (4) | Mg2—Ow5 | 2.068 (4) |
| Mg1—Ow1 | 2.131 (4) | Mg2—O5 | 2.124 (4) |
| Mg3—O3 | 2.046 (4) | Mg3—Ow3 | 2.087 (5) |
| Mg3—O2 | 2.061 (4) | Mg3—Ow6 | 2.092 (5) |
| Mg3—Ow4 | 2.074 (4) | Mg3—Ow2 | 2.098 (4) |
| P1—O4 | 1.621 (4) | P2—O4 | 1.620 (4) |
| P1—O6 | 1.493 (4) | P2—O1 | 1.504 (4) |
| P1—O3 | 1.507 (4) | P2—O5 | 1.507 (4) |
| P1—O7 | 1.518 (4) | P2—O2 | 1.520 (4) |

Valence angles (°) and O···O distances (Å)

| | | |
|---|---|---|
| O1—Mg1—O6 | 87.6 (2) | 2.844 (5) |
| O1—Mg1—Ow1 | 89.2 (2) | 2.925 (6) |
| O6—Mg1—Ow1 | 88.9 (2) | 2.948 (6) |
| O3—Mg3—O2 | 93.3 (2) | 2.978 (5) |
| O3—Mg3—Ow4 | 89.8 (2) | 2.909 (6) |
| O3—Mg3—Ow3 | 93.2 (2) | 3.003 (6) |
| O3—Mg3—Ow6 | 94.7 (2) | 3.044 (7) |
| O3—Mg3—Ow2 | 176.6 (2) | |
| O2—Mg3—Ow4 | 94.8 (2) | 2.847 (6) |
| O2—Mg3—Ow3 | 173.5 (2) | |
| O2—Mg3—Ow6 | 91.3 (2) | 2.882 (6) |
| O7—Mg2—Ow5 | 89.7 (2) | 2.915 (6) |
| O7—Mg2—O5 | 86.5 (2) | 2.870 (5) |
| Ow5—Mg2—O5 | 89.4 (2) | 2.949 (6) |
| O2—Mg3—Ow2 | 85.1 (2) | 2.812 (5) |
| Ow4—Mg3—Ow3 | 85.2 (2) | 2.815 (7) |
| Ow4—Mg3—Ow6 | 172.2 (2) | |
| Ow4—Mg3—Ow2 | 87.4 (2) | 2.881 (6) |
| Ow3—Mg3—Ow6 | 88.3 (2) | 2.910 (7) |
| Ow3—Mg3—Ow2 | 88.4 (2) | 2.918 (6) |
| Ow6—Mg3—Ow2 | 88.3 (2) | 2.917 (6) |
| P1—O4—P2 | 125.6 (2) | |
| O4—P1—O6 | 104.9 (2) | 2.469 (5) |
| O4—P1—O3 | 105.9 (2) | 2.497 (5) |
| O4—P1—O7 | 106.0 (2) | 2.507 (5) |
| O6—P1—O3 | 113.4 (2) | 2.507 (5) |
| O6—P1—O7 | 113.9 (2) | 2.524 (5) |
| O3—P1—O7 | 111.9 (2) | 2.506 (5) |
| O4—P2—O1 | 102.8 (2) | 2.443 (5) |
| O4—P2—O5 | 107.1 (2) | 2.516 (5) |
| O4—P2—O2 | 106.6 (2) | 2.518 (5) |
| O1—P2—O5 | 115.5 (2) | 2.547 (5) |
| O1—P2—O2 | 111.8 (2) | 2.505 (5) |
| O5—P2—O2 | 112.1 (2) | 2.511 (5) |

O—Mg—O angles range from 85.2 to 94.8°, and the *trans* angles from 172.2 to 180.0°. In the $O_3POPO_3^{4-}$ anion, the two bridging P—O distances are equal to 1.620 Å, and the terminal P—O distances range from 1.493 to 1.520 Å. Most of the variation in P—O bond lengths corresponds to off-center displacements of the central P atoms within relatively regular tetrahedra of O atoms. The sample averages and e.s.d.'s are 1.536 ± 0.053 Å for the P—O bond lengths and 2.504 ± 0.026 Å for the tetrahedral O···O distances. Thus the P—O variation is about twice as large as the O···O variation. The bridging P—O—P angle is 125.6°. The O—P—O angles between the bridging and terminal O atoms range from 102.8 to 107.1°; the O—P—O angles between terminal O atoms are larger and range from 111.8 to 115.5°. The conformation of the anion is within ~10° of being eclipsed. In the water molecules, O—H distances range from

Table 3. *Geometries of* O—H···O, O—H(···O)$_2$ *and* O(—H···)$_2$O *interactions in* $Mg_2P_2O_7.6H_2O$ *crystals*

E.s.d.'s average 0.007 Å for O···O, 0.07 Å for O—H and H···O, and 5° for O—H···O.

| | O—H (Å) | | H···O (Å) | O···O (Å) | O—H···O (°) | Symmetry* | Translation |
|---|---|---|---|---|---|---|---|
| Ow1—H11 | 0.84 | Ow1 | 2.78 | 3.16 | 109 | (2) | 1 0 0 |
| | | O1 | 2.96 | 2.92 | 79 | (2) | 0 0 0 |
| H12 | 0.75 | O5 | 2.10 | 2.80 | 155 | (1) | 0 0 0 |
| | | O7 | 2.70 | 3.22 | 127 | (2) | 1 0 1 |
| | | Ow1 | 2.87 | 3.16 | 105 | (2) | 1 0 0 |
| Ow2—H21 | 0.97 | Ow1 | 1.86 | 2.79 | 160 | (4) | 0 0 0 |
| | | O7 | 2.64 | 3.11 | 110 | (3) | −1 0 −1 |
| | | Ow5 | 2.72 | 2.83 | 86 | (4) | 0 0 0 |
| H22 | 1.00 | O3 | 1.74 | 2.74 | 178 | (3) | −1 0 −1 |
| | | O7 | 2.57 | 3.11 | 114 | (3) | −1 0 −1 |
| Ow3—H31 | 0.89 | O5 | 2.29 | 3.14 | 157 | (3) | −1 0 0 |
| | | Ow5 | 2.39 | 2.93 | 119 | (4) | 0 0 1 |
| H32 | 0.88 | O1 | 2.07 | 2.87 | 150 | (3) | 0 0 0 |
| | | Ow5 | 2.55 | 2.93 | 106 | (4) | 0 0 1 |
| Ow4—H41 | 0.71 | O2 | 2.15 | 2.85 | 162 | (3) | 0 0 0 |
| | | O1 | 2.75 | 3.06 | 108 | (3) | 0 0 0 |
| | | Ow6 | 2.94 | 3.36 | 110 | (1) | 1 0 0 |
| H42 | 1.00 | O6 | 1.86 | 2.80 | 154 | (3) | 0 0 −1 |
| | | O3 | 2.56 | 3.35 | 134 | (3) | 0 0 −1 |
| | | Ow6 | 2.94 | 3.36 | 106 | (3) | 0 0 −1 |
| | | O1 | 2.95 | 3.06 | 86 | (3) | 0 0 0 |
| Ow5—H51 | 1.01 | Ow2 | 1.84 | 2.83 | 166 | (4) | 0 −1 0 |
| | | O7 | 2.82 | 2.93 | 85 | (2) | 1 0 1 |
| | | Ow6 | 2.91 | 3.34 | 106 | (2) | 0 0 1 |
| H52 | 0.72 | O4 | 2.13 | 2.81 | 161 | (2) | 0 0 1 |
| | | O6 | 2.86 | 3.31 | 123 | (2) | 0 0 1 |
| Ow6—H61 | 0.84 | O3 | 2.58 | 3.33 | 149 | (3) | −1 0 −1 |
| | | Ow3 | 2.63 | 3.29 | 136 | (3) | −1 0 −1 |
| | | Ow4 | 2.79 | 3.36 | 121 | (1) | −1 0 0 |
| H62 | 0.92 | O2 | 2.04 | 2.88 | 151 | (3) | −1 0 0 |
| | | Ow2 | 2.69 | 3.37 | 132 | (3) | −1 0 0 |
| | | Ow4 | 2.75 | 3.36 | 124 | (3) | −1 0 0 |

* Symmetry-equivalent positions: (1) $x, y, z$; (2) $-x, -y, -z$; (3) $\frac{1}{2}+x, \frac{1}{2}-y, \frac{1}{2}+z$; (4) $\frac{1}{2}-x, \frac{1}{2}+y, \frac{1}{2}-z$.

0.71 to 1.01 Å, and H—O—H angles from 96 to 118°. Bond-length and valence-angle e.s.d.'s average 0.004 Å and 0.2° for the non-H structure, and 0.06 Å and 4° for bonds to H atoms.*

*Comparisons among the hexahydrate, dihydrate, and α- and β-anhydrous structures*

All of the structures can be viewed as being built up of $MgO_6$ octahedra and vertex-sharing pairs of $PO_4$ tetrahedra. There is no face or vertex sharing between octahedra, nor any face or edge sharing between octahedra and tetrahedra, in any of the structures. In all of the structures, all vertices of the $PO_4$ tetrahedra are shared: the P—O—P bridging vertex between the pairs of tetrahedra, and the terminal vertices with $MgO_6$ octahedra. Thus the terminal P—O oxygens always coordinate $Mg^{2+}$ cations, but the bridging P—O—P oxygens never do. The four crystal structures are illustrated in Figs. 2–5, with the unit cells of the densely packed dihydrate and anhydrous crystals 'exploded' to separate the octahedra and tetrahedra.

* Tables of anisotropic mean-square-displacement parameters, bond-length-normalized (0.96 Å O—H) H-atom coordinates, structure-factor magnitudes, stereoscopic versions of all the structure diagrams, and summaries of structural data for other representative pyrophosphate and magnesium phosphate structures have been deposited with the British Library Document Supply Centre as Supplementary Publication No. SUP 54738 (18 pp.). Copies may be obtained through The Technical Editor, International Union of Crystallography, 5 Abbey Square, Chester CH1 2HU, England. [CIF reference: CR0338]

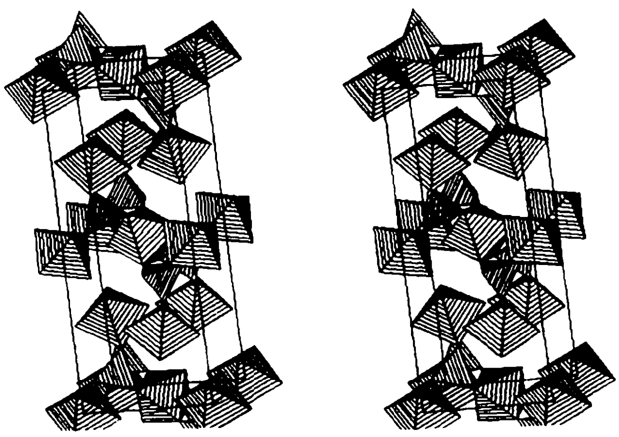

Fig. 2. Packing of the $MgO_6$ octahedra and $O_3POPO_3^{4-}$ pairs of tetrahedra in the unit cell of $Mg_2P_2O_7.6H_2O$. The *b* axis is approximately vertical, and the *a* axis horizontal. The pair of tetrahedra and their attached octahedra in the lower left of the diagram correspond to a crystal-chemical unit as illustrated in Fig. 1.

The hexahydrate crystals have the smallest mass density and the most open structure. In the hexahydrate the octahedra are discrete, but in all the other structures the octahedra share two or more edges. In the dihydrate (Oka & Kawahara, 1982) and in the $\alpha$-anhydride (Calvo, 1967), octahedra share edges to form infinite zigzag chains, which are cross-linked through the tetrahedra *via* shared vertices. In the $\beta$-anhydride (Calvo, 1965), rings of six octahedra are formed by edge sharing, and each ring is linked to two neighboring rings, also by edge sharing. Only pyrophosphate oxygens are shared in the Mg—O—Mg bridges between octahedra; each water molecule in the hydrate structures ligates only one magnesium ion.

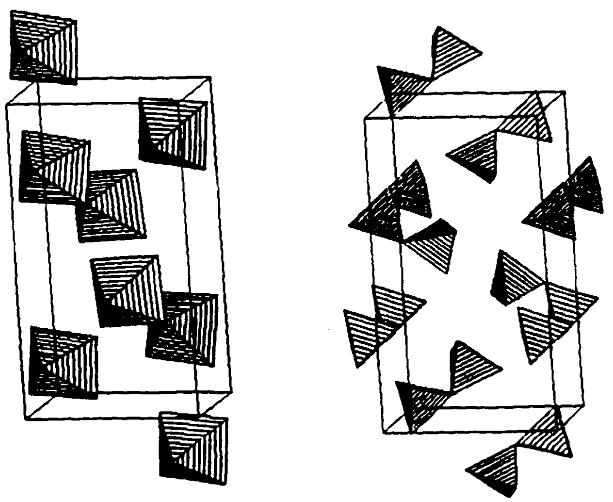

Fig. 3. Unit-cell drawings for the $Mg_2P_2O_7.2H_2O$ crystal structure [monoclinic, $P2_1/n$, $a = 7.367\,(1)$, $b = 13.906\,(3)$, $c = 6.277\,(1)$ Å, $\beta = 94.37°$, $V = 641.2$ Å$^3$, $Z = 4$, $D_x = 2.66$ mg mm$^{-3}$ (Oka & Kawahara, 1982)]. For clarity, the $MgO_6$ octahedra and $O_3POPO_3^{4-}$ pairs of tetrahedra are drawn separately. The $b$ axis is approximately vertical, and the $c$ axis horizontal.

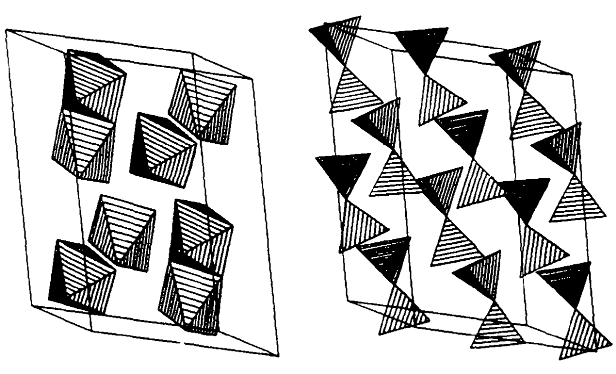

Fig. 4. Unit-cell drawings for the $\alpha$-$Mg_2P_2O_7$ crystal structure [$T = 295$ K, monoclinic, $B2_1/c$ (nonstandard $B$-centered cell chosen for the sake of comparison with the high-temperature $\beta$-phase), $a = 13.198\,(10)$, $b = 8.295\,(5)$, $c = 9.072\,(4)$ Å, $\beta = 104.9\,(1)°$, $V = 959.8$ Å$^3$, $Z = 8$, $D_x = 3.18$ mg mm$^{-3}$ (Calvo, 1967)]. For clarity the $MgO_6$ octahedra and $O_3POPO_3^{4}$ pairs of tetrahedra are drawn separately. The $a$ axis is approximately vertical, and the $c$ axis horizontal.

The geometries of the $MgO_6$ octahedra tend to be more regular in the hydrates than in the anhydrides. Octahedral distortion reaches an extreme in the $\beta$-anhydride (Calvo, 1965), in which the Mg—O distances range from 2.06 to 2.14 Å in the one octahedron, but from 1.99 to 2.12 to 3.35 Å in the other 'octahedron'. The latter is perhaps better described as a distorted square pyramid, which shares a pair of edges with two neighboring octahedra, and shares one vertex and has a 3.35 Å non-bonded Mg—O contact with a third octahedron.

Pyrophosphate groups are conformationally flexible about the two P—O bonds of the central P—O—P bridge, and have, in principle, five possible idealized conformations: a pair of staggered and eclipsed conformations about a linear P—O—P link, and three conformations – one staggered and two eclipsed – about a bent link, as sketched in Fig. 6. As discussed below, a linear P—O—P link probably has only transitory existence. There appears to be no systematic nomenclature for the several pyrophosphate conformations about a bent P—O—P link.

In the two hydrates, the $P_2O_7^{4-}$ anions have very similar bent, nearly eclipsed conformations (II, Fig. 6), and each anion binds two $Mg^{2+}$ cations in a bidentate chelate manner, and a pair of cations in a monodentate manner. In the two anhydrides, the anions assume staggered conformations (I and IV, Fig. 6), and each anion binds six cations in a monodentate manner. The average of the P—O bond lengths in the P—O—P bridges is 1.614 Å for the eclipsed conformations in the two hydrate structures, and 1.590 Å for the staggered conformation in the $\alpha$-anhydride. The P—O—P angle is 126° in the hexahydrate and dihydrate, and 144° in the $\alpha$-anhydride. Thus in the eclipsed conformation the

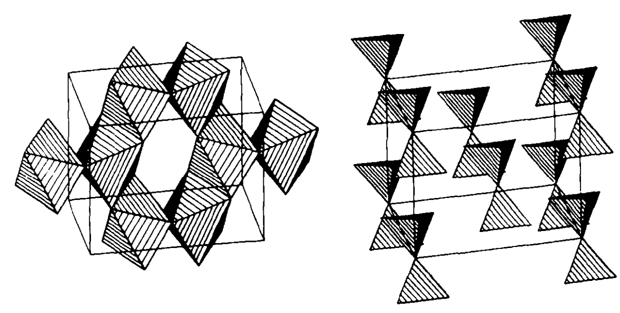

Fig. 5. Unit-cell drawings for the $\beta$-$Mg_2P_2O_7$ crystal structure [$T = 368\,(5)$ K, monoclinic, $C2/m$, $a = 6.494\,(7)$, $b = 8.28\,(1)$, $c = 4.522\,(5)$ Å, $\beta = 103.8\,(1)°$, $V = 236.1$ Å$^3$, $Z = 2$, $D_x = 3.23$ mg mm$^{-3}$ (Calvo, 1965)]. For clarity, the $MgO_6$ octahedra and $O_3POPO_3^{4}$ pairs of tetrahedra are drawn separately. The $a$ axis is approximately vertical, and the $b$ axis horizontal.

P—O—P bridge is bent by almost 20°, and the bridging P—O bonds are stretched by $\sim 0.02$ Å, as compared with the staggered conformation. Analogous, but smaller, differences between the P—O—P bridge geometries occur in a number of other examples of eclipsed and staggered pyrophosphate conformations in crystals, which are tabulated in the deposited supplementary publication material. The differences are larger for the magnesium pyrophosphate structures because of the small ionic radius of magnesium, and because, in the hydrate crystals, each anion binds as a bidentate chelating ligand to two aqua cations simultaneously.

### *The question of a linear* P—O—P *bridge*

In $\beta$-$Mg_2P_2O_7$ (Calvo, 1965), the bridging oxygen occupies an apparent crystallographic center of symmetry, so that the P—O—P bridge is apparently linear, with P—O bond lengths foreshortened to 1.557 Å. The mean-square displacement of the bridging oxygen is, however, strongly anisotropic and more than five times larger than the mean-square displacements of the terminal oxygens. It therefore seems that the apparently linear structure is a centrosymmetric average of disordered bent structures.

The diffraction data for $\beta$-$Mg_2P_2O_7$ were eye-estimated film data [$R(|F|) = 0.15$ for 488 data to $(\sin\theta_{\max})/\lambda \simeq 0.4$ Å$^{-1}$ with Mo $K\alpha$ radiation]. The $\beta$-phase was maintained above the phase transition temperature by heating the crystal to $368 \pm 5$ K with a hair dryer inserted along the axis of the Weissenberg camera. Under these circumstances, the photographic exposure times were kept rather short, and only 340 of the 488 measured reflections were classed as observed above background. The choice of the centrosymmetric space group $C2/m$ was based on electron paramagnetic resonance measurements with $Mn^{2+}$-doped crystals. Though resourceful, these experiments do not resolve the problem of disorder of the P—O—P bridging oxygen in the high-temperature $\beta$-phases of pyrophosphates of $Mg^{2+}$, $Mn^{2+}$, $Cu^{2+}$ and $Zn^{2+}$, which are isostructural with thortveitite (Robertson & Calvo, 1968). There is thus no convincing evidence for a linear P—O—P bridge, which presumably can have only transitory existence.

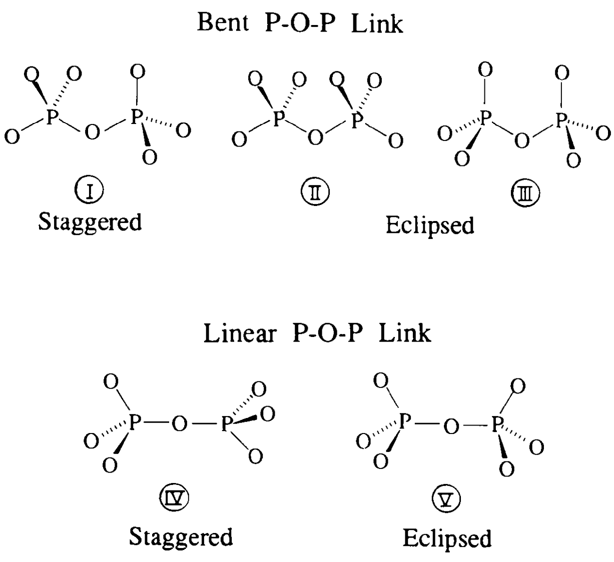


Fig. 6. Idealized possible conformations for pyrophosphate anions. Bidentate chelating ligation to a metal ion is possible only for the eclipsed conformations labeled (II) and (III), which are presumably, for an isolated anion, high-energy conformations about a bent P—O—P link. Stable existence of a linear P—O—P link is doubtful.

### *The role of* $Mg^{2+}$ *as a cofactor in ATP–ADP bioenergetics*

The $Mg_2P_2O_7.nH_2O$ structures show the strong tendency of the magnesium ion for sixfold octahedral coordination of oxygen, and they indicate that in an aqueous environment the preferred mode of ligation of pyrophosphate to the magnesium ion is bidentate chelation. This is the mode of binding that has been proposed for the participation of the magnesium ion as a cofactor in exergonic ATP and ADP hydrolyses that drive endergonic biochemical reactions (see, *e.g.*, Merritt & Sundaralingam, 1980). Evidently, the $Mg^{2+}$ cation neutralizes like-charge repulsions within the polyphosphate polyanions, and acts as a template for binding bidentate diphosphate or tridentate triphosphate groups in eclipsed conformations. As shown above, these chelate conformations close the bridging P—O—P valence angle, stretch the bridging P—O bonds, and maximally expose the bridging oxygen for hydrolytic scission of the P—O—P link. The *cis*-$(H_2O)_4MgO_2$ bidentate coordination at Mg3 in the hexahydrate structure (Fig. 1) provides a particularly clear example of this chemical geometry.

Crystals of binary Mg–ATP or Mg–ADP complexes have been notoriously difficult to obtain, because the complexes are labile and undergo spontaneous nonenzymic hydrolysis. Crystals of stable ternary complexes with 2,2′-dipyridylamine have, however, been studied, along with binary complexes of ATP or ADP with various divalent cations other than $Mg^{2+}$ (Sabat, Cini, Haromy & Sundaralingam, 1985, and references cited therein). These studies confirm the tendency to polydentate polyphosphate chelation that bends, stretches, and exposes the P—O—P bridge, and they indicate that Nature's choice of $Mg^{2+}$ as a cofactor in ATP–ADP bioenergetics represents a judicious balance between the stability of the $\overline{\text{MgOPOPO}}$ chelate ring and stereochemical exposure of the P—O—P link to hydrolytic attack. The particular effectiveness of $Mg^{2+}$ as a template for chelate binding of ATP and ADP, bending the P—O—P link and exposing the bridging oxygen, is attributable to the cation's relatively small ionic radius and large charge-to-radius ratio. Among the cations that are present in the biological milieu in greater than trace amounts, namely, the so-called bulk metals, $Na^+$, $K^+$, $Ca^{2+}$ and $Mg^{2+}$, the magnesium ion is the smallest.

We are grateful for technical help from Mr Brian Tucker (Buffalo) and Monsieur Daniel Bayeul (Nancy), and for research support from USDHHS PHS NIH grant No. GM34073. RHB is grateful for the hospitality of the Laboratoire de Cristallographie à le Université de Nancy during a three-month visiting professorship in the Spring of 1988.

### References

BLESSING, R. H. (1989). *J. Appl. Cryst.* **22**, 396–397, and references cited therein.
CALVO, C. (1965). *Can. J. Chem.* **43**, 1139–1146.
CALVO, C. (1967). *Acta Cryst.* **23**, 289–295.
CROMER, D. T. & WABER, J. T. (1974). *International Tables for X-ray Crystallography*, Vol. IV, edited by J. A. IBERS & W. C. HAMILTON, Table 2.2B, pp. 99–102. Birmingham: Kynoch Press. (Present distributor Kluwer Academic Publishers, Dordrecht.)
FISCHER, R. X. (1985). *J. Appl. Cryst.* **18**, 258–262.
FRENCH, S. & WILSON, K. (1978). *Acta Cryst.* A**34**, 517–525.
GABE, E. J., LEE, F. L. & LE PAGE, Y. (1985). *Crystallographic Computing* 3, edited by G. M. SHELDRICK, C. KRÜGER & R. GODDARD, pp. 164–174. Oxford: Clarendon Press.
JOHNSON, C. K. (1970). *ORTEP*. Report ORNL-3794, 2nd revision. Oak Ridge National Laboratory, Tennessee, USA.
LUKASZEWICZ, K. (1961). *Rocz. Chem.* **35**, 31. [As cited by Calvo (1967).]
LUKASZEWICZ, K. (1967). *Bull. Acad. Pol. Sci. Ser. Chim.* **15**, 53. [As cited by Calvo (1967).]
MERRITT, E. A. & SUNDARALINGAM, M. (1980). *Acta Cryst.* B**36**, 2576–2584.
MOTHERWELL, S. (1970). *PLUTO*. Program for plotting molecular and crystal structures. Univ. of Cambridge, England.
OKA, J. & KAWAHARA, A. (1982). *Acta Cryst.* B**38**, 3–5.
ROBERTSON, B. E. & CALVO, C. (1968). *Can. J. Chem.* **46**, 605–612.
SABAT, M., CINI, R., HAROMY, T. & SUNDARALINGAM, M. (1985). *Biochemistry*, **25**, 7827–7833.
SHELDRICK, G. M. (1976). *SHELX76*. Program for crystal structure determination. Univ. of Cambridge, England.
STEWART, R. F., DAVIDSON, E. R. & SIMPSON, W. T. (1965). *J. Chem. Phys.* **42**, 3175–3181.

*Acta Cryst.* (1992). B**48**, 376–389

# Symmetry Determination and Pb-Site Ordering Analysis for the $n = 1, 2$, $Pb_xBi_{2-x}Sr_2Ca_{n-1}Cu_nO_{4+2n+\delta}$ Compounds by Convergent-Beam and Selected-Area Electron Diffraction

BY P. GOODMAN
*School of Physics, University of Melbourne, Parkville, Australia* 3052

P. MILLER
*Division of Materials Science and Technology, CSIRO, Locked Bag* 33, *Clayton, Australia* 3188

T. J. WHITE
*Electron Microscope Centre, University of Queensland, St Lucia, Queensland, Australia* 4076

AND R. L. WITHERS
*Research School of Chemistry, Australian National University, GPO Box* 4, *Canberra, Australia* 2601

(*Received* 9 *September* 1991; *accepted* 3 *February* 1992)

### Abstract

An examination of various preparations from the structural series $Pb_xBi_{2-x}Sr_2Ca_{n-1}Cu_nO_{4+2n+\delta}$ by selected-area and convergent-beam electron diffraction (SAD and CBED) shows that despite superstructural symmetries which range from monoclinic to orthorhombic, space groups *Amaa* or *A2aa* can be unambiguously identified for the subcells of different samples (here for $n = 1$ and $n = 2$ respectively), independently of the long-range superstructural result. An analysis of the $n = 2$ compound within the compositional range $x = 0.2 \rightarrow 0.3$ shows that both Pb-independent and Pb-dependent superlattices coexist for this range of $x$, the former superlattice retaining the superspace-group symmetry of

0108-7681/92/040376-14$06.00